DEFECTS IN ELECTRON-IRRADIATED IRON-DOPED SILICON

S.H. Muller, H.G. Arnold, J.J. de Graaf, G.M. Tuynman and C.A.J. Ammerlaan,

Natuurkundig Laboratorium, Universiteit van Amsterdam, Valckenierstraat 65, 1018 XE Amsterdam, The Netherlands

High-resistivity n-type silicon containing neutral interstitial iron was irradiated with 1.8 MeV electrons. Several defects thereby produced were observed in electron paramagnetic resonance. The spectra are complex and up to the present only the patterns of two predominant defects could be isolated and analyzed. The defects have <111> axial symmetry. Their identification with substitutional iron and with the iron-divacancy pair is considered. The spectra are unstable at room temperature.

1. Introduction.

Only recently it has become known that iron is often unintentionally present as an impurity in silicon crystals. Since interstitial iron has a high mobility in silicon at normal temperatures it is readily involved in defect interaction processes. The present paper reports on the behaviour of iron in silicon in which primary lattice defects (vacancies, divacancies, and self interstitials) were produced by electron irradiation. Many previous studies have demonstrated that vacancies in silicon are trapped by substitutional donors /1,2/, acceptors /3,4/, and the isoelectronic impurities: germanium /5/ and tin /6/. Interstitial impurities, such as oxygen /7/ and the transition metals chromium and manganese /8/, also act as vacancy traps. Often these defect associations are quite stable.

Iron can be trapped interstitially near substitutional impurities to form impurity pairs. The formation of acceptor-iron /9/ and gold-iron /10/ pairs is well established; the existence of iron-iron pairs has been proposed /10/.

2. Experiment.

Samples were prepared by diffusion of iron into 118 Ohm.cm

phosphorus-doped silicon. The silicon was grown by the floating-zone method and was specified to be dislocation-free. Iron impurities were uniformly distributed through the samples, of typical dimensions of $15 \times 2 \times 2$ mm^3, by keeping them at $\simeq 1200^{\circ}$C for one hour. This heat-treatment was followed by a fast quench of the samples into water. Irradiations with 1.8 MeV electrons from a Van de Graaff accelerator were performed at room temperature. The dose of 6×10^{17} electrons per cm^2 was given in $\simeq 6$ hours. Heat dissipation of the electron beam raised the temperature of the sample by less than 30°C. For the purpose of mounting the sample in the microwave cavity, using bees wax, the sample temperature was raised to $\simeq 70^{\circ}$C for some minutes. Because remounting proved necessary in the course of the measurements this had to be repeated a few times. For the electron paramagnetic resonance studies we used our 23 GHz superheterodyne spectrometer which was tuned to observe the dispersive part of the magnetic susceptibility. Best signals were generally obtained with sample temperatures from 1 to 4.2 K.

3. Results.

In the samples a rich variety of electron paramagnetic resonance spectra is observed. The spectra are not stable when keeping the sample at room temperature. This implies that new defects are created, that existing defects are annihilated, or that spectra (dis)appear as a shift of the Fermi level makes a defect (un)observable. A detailed systematic study of these phenomena has not yet been made. With the presently available data the main effects are summarized as follows.

Immediately after heat-treatment at 1200°C a strong spectrum associated with isolated neutral iron atoms in interstitial positions of the silicon lattice is observed. This well-known resonance of Fe_i° /9,11/, described by an isotropic g-value $g = 2.0699$, generally has a linewidth less than 0.3 mT. After electron irradiation the line remains strongly present in all subsequent stages.

Upon irradiation the dominant radiation spectrum observed corresponds to a defect with $J = 3/2$. The angular dependence of the six patterns associated with transitions between the four spin levels is shown in figure 1. The patterns reveal $\langle 111 \rangle$ axial symmetry for the defect. The spectrum is accurately described by the spin-Hamiltonian

$$H = g_{//}\mu_B B_z J_z + g_{\perp}\mu_B(B_x J_x + B_y J_y) + D\left[J_z^2 - \tfrac{1}{3}J(J+1)\right],$$

in the own principal axes system of each defect.

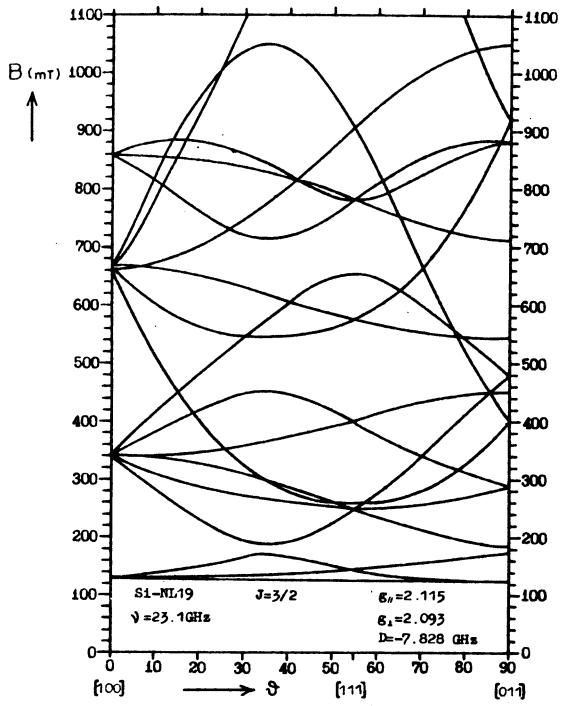

Fig. 1. Angular dependence of the Si-NL19 spectrum with B in the (011) - plane.

The spin-Hamiltonian constants as determined by a computer fit are given in Table 1. The spectrum, hitherto not reported, is labelled Si-NL 19. The intensity of the NL19-spectrum is about one tenth of that of the Fe_i^o- spectrum, while it is stronger than the usual radiation damage centers with g-values between 2.00 and 2.01. Though the NL19-intensity is amply sufficient to raise ^{29}Si hyperfine lines above the noise level, these are not observed. Apparently, they are not resolved from the main lines, whose widths are between 0.2 and 0.5 mT.
Also present is the isotropic spectrum with g = 3.524 corresponding to positively charged interstitial iron /9,11-14/. The intensity of this spectrum, which was completely absent before irradiation, reaches about 5% of the neutral iron amplitudes.

After an anneal treatment at $\simeq 70^{\circ}C$ for $\simeq 5$ minutes the intensity of the NL19-spectrum was reduced to about one quarter of the pre-anneal value. Compensating for this loss a large number of new resonances had emerged. The complex spectra, whose analysis will be quite laborious,

were not recorded in sufficient detail when they were lost in a second unintentional anneal at $\simeq 70^{o}C$ for $\simeq 5$ minutes. Besides NL19 and a number of other lines, the prominent spectrum present after this anneal characterized a new defect again having $\langle 111 \rangle$ axial symmetry. The parameters describing this NL20-spectrum are given in Table 1. Spectrum Si-A22, observed by Lee et al. /10/ in slowly-quenched samples, was not present.

Table 1. Spin-Hamiltonian parameters of selected EPR-spectra related to iron in silicon.

Defect	Spectrum	J	$g_{//}$	$g_{\perp}$	D (GHz)	References
Fe_i^+		1/2	3.524	isotropic	-	9,11-14
Fe_I^o		1	2.0699	isotropic	0	9,11
	A22	1/2	2.1001	4.0264	-	10
		3/2	2.1001	2.0132	$\gg 9$	
	NL19	3/2	2.115	2.093	-7.828	-
			± 0.001	± 0.001		
	NL20	1/2	2.064	6.22	-	-
		5/2*	2.064	2.075	$\gg 23$	
			± 0.003	± 0.003		
$(Fe_iB_s)^o$		3/2	2.068	2.0	$\gg 30$	9**
$(Fe_iAu_s)^o$	A23	1/2	2.1001	2.1178	-	10**

* Preferred set of parameters, calculated by taking the cubic field splitting constants a and a-F equal to zero in analysis.
** Complete set of parameters in reference.

4. Discussion.

A highly succesful model was proposed by Ludwig and Woodbury to account for the observed properties of interstitial and substitutional transition metal imourities in silicon /13/. The application of this model to the case of substitutional iron in silicon is illustrated in figure 2. Four elec-

trons of the iron atom are transferred to the valence shell to form covalent bonds with the nearest-neighbour silicon

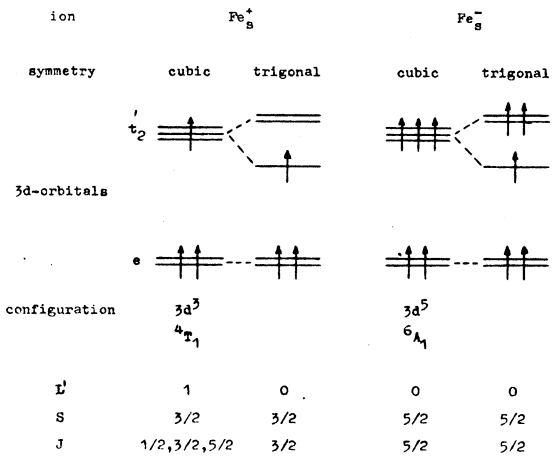

Fig. 2. Electronic structure of positive (left part) and negative (right part) substitutional iron in silicon.

atoms. This leaves positive iron in a $3d^3$- configuration, while negative iron has 5 electrons in the 3d-shell. The d-levels, split by the tetrahedral crystalline field into doublet e-states and higher lying triplet t_2 - states, are filled in accordance with Hunds' s rule to obtain maximum spin S. According to the model positive iron has an orbitally degenerate $^4T_1$ ground state and is liable therefore to Jahn-Teller distortion. This will lower the symmetry of the center, possibly to trigonal. The $^6A_1$ ground state of negative iron is only spin degenerate and no measurable Jahn-Teller effect is to be expected. Nevertheless, it is conceivable that a true off-center position of the iron ion is energetically favoured as it may lead to more stable hybrid orbitals with the nearest-neighbour silicon atoms.

The radiation-induced iron-related defects, A22 and our centers NL19 and NL20, all exhibit trigonal symmetry. In this experimentally established lower-than-cubic symmetry the degeneracy of the triplet states is lifted and the associated effective orbital momentum is quenched. The remaining angular momentum is therefore pure spin, resulting in spin $J = \frac{1}{2} n$, where n is the number of unpaired 3d - electrons. One thus expects $J = \frac{3}{2}$ for Fe_s^+, and $J = \frac{5}{2}$ for Fe_s^-. For the FeB and FeAu - spectra, which likewise have trigonal symmetry, this approach leads to spins $J = \frac{3}{2}$ and $J = \frac{1}{2}$, respectively, as reported by Ludwig and Wood-

bury /9/ and Lee et al. /10/. The corresponding predicted g-factors are nearly isotropic and close to the spin g-value g = 2. For FeB and FeAu such values have been reported /9,10/.

Experimentally for the spectra A22 and NL20 only one pattern is observed with strongly anisotropic effective g-value. When analyzing these patterns with $J = \frac{1}{2}$ the values $g_\perp = 4.0264$ and 6.22 respectively, as shown in Table 1. are obtained. In an alternative analysis the observed resonances can be considered as the transition between lowest levels belonging to a higher spin multiplet. Due to a large zero-field splitting parameter D the separation between ground state levels and excited states may be large compared to the microwave quantum of the resonance experiment. For instance, a trigonal field will split a cubic ^6S- state into three doublets. Experimental observation of the transitions in the higher doublets is hampered by their lower occupation (Boltzmann factor and their generally smaller transition probabilities. In the case of large splitting the analysis according to the parameters given on the second lines in Table 1 for spectra A22 and NL20 is mathematically equivalent as far as ground state transitions are concerned. This second set of parameters is physically much more appealing.

Primarily on the basis of spin values the identification of spectra NL19 or A22 with positive substitutional iron Fe_s^+ and spectrum NL20 with negative substitutional iron Fe_s^- may be proposed. The g-factors of the defects slightly deviate from the free electron value g = 2.0023. The g-shift of the irradiation defects is equal in sign and comparable in magnitude to that of neutral interstitial iron. This might be explained in a crystal field approach by having a comparable mixing of excited states into the ground level by spin-orbit interaction.

Another possibility for defect formation is trapping of mobile interstitial iron in an irradiation produced divacancy. In a defect model analogous to that established for the tin-vacancy pair /6/ the iron ion could reside in a position halfway between the silicon atom sites. Six electrons are needed to occupy the hybrid orbitals giving bonding to the nearest-neighbour atoms. In the negative charge state three electrons are left in the 3d-shell. The resulting spin $J = \frac{3}{2}$ and the 3m point group symmetry of the defect are compatible with spectra NL19 and A22.

Identification of spectrum NL19 with Fe_s^+ and spectrum A22 with $(Fe_i + V_2)^-$ is consistent with the high pro-

duction rate observed for NL19, and is identical with the assignment for A22 made by Lee et al. /10/. In this view the spectra NL19 and NL20 are related to one defect structure, in different charge states. The simultaneous observation of both spectra leaves some doubt about the validity of this interpretation.

The absence of resolved ^{29}Si hyperfine interactions in spectrum NL19 indicates a low probability for the defect electrons on the neighbouring silicon atoms. An interpretation of the zero-field splitting constant D should therefore be based on interactions between electrons largely localized on the iron atom. If the coupling arises via spin-orbit interaction, then, according to Pryce /15/, the relation $D = \frac{1}{2}\lambda(g_{//} - g_{\perp})$ will hold. Applying this to spectrum NL19, and substituting $D = -7.828$ GHz and $g_{//} - g_{\perp} = 0.022$, one arrives at a spin-orbit coupling constant $\lambda = \mp 24\ cm^{-1}$. The order of magnitude of λ is correct for iron and the minus sign is consistent with a positive g-shift. On the other hand, a negative value for λ indicates a more than half filled d-shell, which is hard to reconcile with iron in a substitutional position. However, also in previous cases the use of Pryce's expression relating D to g-anisotropy has met difficulties /3,6/.

The identifications as discussed must at present be considered as tentative. More systematic work on these centers, including hyperfine studies with ^{29}Si and ^{57}Fe and response to applied stress, should provide data on which more reliable atomic models can be based.

References.

1. G.D. Watkins and J.W. Corbett, Phys. Rev. 134, A1359 (1964)
2. E. Elkin and G.D. Watkins, Phys. Rev. 174, 881 (1968)
3. G.D. Watkins, Phys. Rev. 155, 802 (1967)
4. G.D. Watkins, Phys. Rev. B13, 2511 (1976)
5. G.D. Watkins, IEEE Trans. Nucl. Sci. NS-16, 13 (1969)
6. G.D. Watkins, Phys. Rev. B12, 4383 (1975)
7. G.D. Watkins and J.W. Corbett, Phys. Rev. 121, 1001 (1961)
8. H.H. Woodbury and G.W. Ludwig, Phys. Rev. Lett. 5, 96(1960)
9. G.W. Ludwig and H.H. Woodbury, Solid State Physics, edited by F. Seitz and D. Turnbull (Academic Press, New York), Vol. 13, p. 223

10. Y.H. Lee, R.L. Kleinhenz, and J.W. Corbett, Defects and Radiation Effects in Semiconductors 1978 (Inst. Phys. Conf. Ser. 46), p. 521
11. H.H. Woodbury and G.W. Ludwig, Phys. Rev. 117, 102 (1960)
12. F.S. Ham, Phys. Rev. A138, 1727 (1965)
13. G.W. Ludwig and H.H. Woodbury, Phys. Rev. Lett. 5, 98 (1960)
14. G.W. Ludwig and H.H. Woodbury, Phys. Rev. 117. 1286 (1960)
15. M.H.L. Pryce, Proc. Phys. Soc. (London) A63, 25 (1950)